










MIN3D Dataset: Multi-seNsor 3D Mapping with an Unmanned Ground Vehicle

Paweł Trybała^{1,3}  · Jarosław Szrek²  · Fabio Remondino³  · Paulina Kujawa¹  · Jacek Wodecki¹  · Jan Blachowski¹  · Radosław Zimroz¹ 

Received: 5 July 2023 / Accepted: 16 September 2023 / Published online: 6 October 2023
© The Author(s) 2023

Abstract

The research potential in the field of mobile mapping technologies is often hindered by several constraints. These include the need for costly hardware to collect data, limited access to target sites with specific environmental conditions or the collection of ground truth data for a quantitative evaluation of the developed solutions. To address these challenges, the research community has often prepared open datasets suitable for developments and testing. However, the availability of datasets that encompass truly demanding mixed indoor–outdoor and subterranean conditions, acquired with diverse but synchronized sensors, is currently limited. To alleviate this issue, we propose the MIN3D dataset (Multi-seNsor 3D mapping with an unmanned ground vehicle for mining applications) which includes data gathered using a wheeled mobile robot in two distinct locations: (i) textureless dark corridors and outside parts of a university campus and (ii) tunnels of an underground WW2 site in Walim (Poland). MIN3D comprises around 150 GB of raw data, including images captured by multiple co-calibrated monocular, stereo and thermal cameras, two LiDAR sensors and three inertial measurement units. Reliable ground truth (GT) point clouds were collected using a survey-grade terrestrial laser scanner. By openly sharing this dataset, we aim to support the efforts of the scientific community in developing robust methods for navigation and mapping in challenging underground conditions. In the paper, we describe the collected data and provide an initial accuracy assessment of some visual- and LiDAR-based simultaneous localization and mapping (SLAM) algorithms for selected sequences. Encountered problems, open research questions and areas that could benefit from utilizing our dataset are discussed. Data are available at <https://3dom.fbk.eu/benchmarks>.

Keywords Robotics · UGV · Underground · Mining · Open dataset · SLAM · Evaluation

✉ Paweł Trybała
ptrybala@fbk.eu; pawel.trybala@pwr.edu.pl

Jarosław Szrek
jaroslaw.szrek@pwr.edu.pl

Fabio Remondino
remondino@fbk.eu

Paulina Kujawa
paulina.kujawa@pwr.edu.pl

Jacek Wodecki
jacek.wodecki@pwr.edu.pl

Jan Blachowski
jan.blachowski@pwr.edu.pl

Radosław Zimroz
radoslaw.zimroz@pwr.edu.pl

¹ Faculty of Geoengineering, Mining and Geology, Wrocław University of Science and Technology (WUST), Wrocław, Poland

² Faculty of Mechanical Engineering, Wrocław University of Science and Technology (WUST), Wrocław, Poland

³ 3D Optical Metrology (3DOM) Unit, Bruno Kessler Foundation (FBK), Trento, Italy

1 Introduction

1.1 Mobile Mapping

Mobile mapping (Chiang et al. 2021; Elhashash et al. 2022) is a widely used technique for various applications, such as documenting and inventorying scenes (Vallet and Mallet 2016; Di Stefano et al. 2021), integration of airborne surveying (Toschi et al. 2017), creating computer models for simulations or decisions (Tak et al. 2021; Feng et al. 2022), and guiding robots for navigation (Funk et al. 2021). The integration of localization and mapping into a single process, known as simultaneous localization and mapping (SLAM), is crucial for accurate spatial positioning and navigation. A variety of sensors and devices can be used for mapping, including 2D and 3D LiDAR scanners, cameras, and depth sensors. SLAM algorithms perform well in indoor environments, such as factories and warehouses, allowing for autonomous operation of robots. However, mapping in outdoor and uncontrolled scenarios presents challenges for SLAM algorithms, such as uneven terrain, limited range of 2D LiDAR sensors, dynamic objects and more sources of sensor noise, which can potentially degrade the quality of mapping and render some popular assumptions useless (e.g., presence of the flat ground). In such scenarios, 3D LiDAR scanners and camera-based systems (V-SLAM) are more effective. In open spaces, global navigation satellite systems (GNSS) can provide a reliable location, but in areas where satellite signals are not available, such as tunnels, caves and mines, a more sophisticated SLAM algorithm is needed.

Research and development of mobile mapping solutions for such environments can be traced back to early works of Thrun et al. (2003), which showcased the usage of laser scanners mounted on a robot to carry out a volumetric 3D survey of an underground mine. Future advances in field robotics and increasing availability of open-source solutions resulted in developing a wide selection of robotic (Kanellakis and Nikolakopoulos 2016; Nüchter et al. 2017; Ren et al. 2019; Trybała 2021; Yang et al. 2022), handheld (Zlot and Bosse 2013; Trybała et al. 2023), and wearable (Masiero et al. 2018; Blaser et al. 2019) solutions of varying complexity for mapping subterranean spaces. However, the problem of performing robust SLAM in challenging environments still cannot be considered as fully solved (Ebadi et al. 2022).

1.2 Open Datasets

To advance research in the field of SLAM, multiple open datasets have been collected and made publicly available

by scientists from the robotics and geomatics communities (Geiger et al. 2012; Liu et al. 2021; Macario Barros et al. 2022; Helmlberger et al. 2022). These datasets allow researchers to investigate various mapping approaches and easily test and evaluate in-house, commercial, or open-source software solutions without the need for access to expensive data acquisition platforms, particularly for robotic systems. The popularity of these datasets has led to the creation of benchmarks, where automated systems evaluate the accuracy of processing methods using standardized metrics and rank them among other submitted solutions.

This approach enables an objective comparison of different SLAM algorithms through use of common metrics, such as absolute and relative trajectory errors (ATE and RTE), to assess localization accuracy. However, there are various other strategies for evaluating the quality of 3D mapping, such as using different metrics for measuring the compliance of point clouds with ground truth (GT), and for aligning the resulting spatial data with reference data, such as using global or local registration methods.

One of the key events that greatly accelerated progress in mobile mapping research were the competitions organized by the US-based Defense Advanced Research Projects Agency (DARPA), such as the DARPA Grand Challenges (starting from 2004) (Seetharaman et al. 2006) and the Subterranean Challenge (held in 2017–2021) (Chung et al. 2023). The former type of competition primarily focused on the needs of the automotive industry, such as localization, mapping, and perception in open, urban areas, and the latter on robot autonomy, perception, and SLAM, respectively. Through dedicated funding, clear goals, and reliable evaluation methods, these events enabled teams from around the world to collaborate and develop innovative SLAM solutions. The by-products of these challenges are also open datasets and benchmarks, which were collected and formed during the field trials of the competitions. Although there are numerous publicly available datasets dedicated to evaluating SLAM algorithms, the diversity of real-world environments in which these algorithms are applied, as well as the various sensor configurations for which mapping solutions are developed, results in a constant need for acquiring more data to evaluate method performance under different conditions. This issue is becoming increasingly critical as learning-based methods gain popularity. Providing them with well-diversified training data with reliable reference data is crucial for their generalization, adaptability, and in consequence usability in real-world scenarios. Furthermore, the universality and uniqueness of a dataset is not only determined by the environment in which the data was collected, but also by the limited set of sensors used. The use of multiple sensors to simultaneously acquire different

types of data not only facilitates the development and testing of data fusion methods, but also provides the most objective way to compare methods based on different sensors, such as visual SLAM (V-SLAM) with LiDAR-based approaches. In recent years, the AMICOS¹ and VOT3D² EIT Raw Materials projects, among others, tackled the use of ground/wheeled/handheld robotic platforms, equipped with various imaging and LiDAR devices, to inspect underground mining scenarios and technical infrastructures. Multi-sensors robots (Trybała et al. 2022) or portable stereo-vision systems (Torresani et al. 2021) can be used to search for hot idlers in a conveyor belt, map underground spaces, or automatically search for humans or damages of components (Szrek et al. 2020; Menna et al. 2022; Dabek et al. 2022).

1.3 Paper Contribution

A common aspect of robotics platforms and mobile mapping solutions is the accuracy and robustness evaluation of localization and mapping methods in harsh conditions (Nocerino et al. 2017; Trybała et al. 2023). Despite the availability of various robotic datasets collected in different environments, most of the available datasets do not have redundant sensor suites or accurate and complete 3D ground truth.

To address the above-mentioned issues, we propose a novel set of data collected in (i) an indoor man-made environment (University buildings) and (ii) an underground facility in Walim (Poland) using a wheeled mobile robot (UGV) equipped with multiple low-cost sensors. The dataset comprises data from an exhaustive, redundant sensor system, including two sets of different stereo cameras, inertial measurement units (IMUs), and two independent LiDAR scanners: a spinning Velodyne VLP-16 with an actuator and a solid-state Livox Horizon. To facilitate the evaluation of mapping results by the users, we also provide reliable GT data in the form of a survey-grade point cloud acquired with a Riegl time-of-flight-based terrestrial laser scanner and the parameters of the external calibration of the sensors mounted on the robot. The collected data are processed and a preliminary accuracy assessment of the results obtained with selected SLAM methods, utilizing various sensors, is presented.

The structure of the article is as follows. First, related works and available datasets for testing SLAM methods are discussed. Then, the utilized in-house mobile robot characteristics, dataset structure, and ground truth data acquisition methodology are presented. The collected and shared eight sequences are reported in Sect. 3, together with some results of the performance of selected state-of-the-art SLAM

algorithms. Finally, the directions of challenging research areas and an outlook or the future developments in the context of utilizing the presented dataset close the paper.

2 Related Works

2.1 SLAM Datasets: Common Scenarios

In the general research area of mobile mapping, numerous open datasets have been published, often featuring a dedicated benchmark. The most prominent research groups involved in these studies focus on the applications in the automotive industry, photogrammetry, surveying, and robotics. At the early days of 3D SLAM developments for autonomous systems, datasets being published were dominated by car-based systems in urban areas and did not focus on benchmarking and metrological evaluation of mapping. Thus, they did not provide an accurate reference data for mapping, but only the raw data from sensor systems consisting usually of camera(s), LiDAR scanners, and inertial measurement unit (IMU) (Smith et al. 2009; Blanco-Claraco et al. 2014; Cordts et al. 2015).

The prime example is the Massachusetts Institute of Technology (MIT) DARPA Grand Challenge 2007 dataset (Huang et al. 2010). Despite the lack of full GT, it still marks an important moment of publicly releasing a huge amount of image and point cloud data, acquired with sensors relevant to the automotive industry applications, enabling a wide audience to work on robotic perception-related solutions. Similarly, two Korea Advanced Institute of Science and Technology (KAIST) datasets (Choi et al. 2018; Jeong et al. 2019) include only GNSS-derived trajectories as the reference data, but provide additional data, recorded at day and at night, and extend the sensor selection by a thermal camera.

Among the most influential SLAM datasets, constituting arguably the most popular benchmark, is the Karlsruhe Institute of Technology and Toyota Technological Institute (KITTI) dataset (Geiger et al. 2012, 2013). The data were collected with a sensor system mounted on a roof of a Volkswagen car in the urban area of Karlsruhe, Germany. Apart from providing image, LiDAR point clouds and IMU data, it includes GNSS-based trajectory and an automated benchmarking system for evaluating the performance of submitted solutions. Although it does not contain a reliable reference for mapping, subsequent developments added other challenges to the benchmark suite, such as image depth prediction, object detection, or semantic segmentation. A recent survey of SLAM algorithms (Liu et al. 2021) highlighted the problem of providing the reliable GT for mapping in open SLAM datasets: only 35 out of 97 investigated datasets include 3D reference data for mapping quality evaluation.

¹ <https://amicos.fbk.eu/>

² <https://vot-3d.com/>

In the robotic and photogrammetric communities, three distinct classes of SLAM datasets can be distinguished, based on whether they were acquired with an unmanned aerial vehicle (UAV), unmanned ground vehicle (UGV), or a handheld system. An example of a UAV-based research is the European Robotics Challenge (EuRoC) dataset (Burri et al. 2016), which features visual–inertial system data with GT data consisting of trajectories acquired with a motion capture (MC) system, total station (TS) tracking and terrestrial laser scanner (TLS) point cloud for mapping evaluation. However, the dataset lacks LiDAR scanning data. For UGV systems, the Technical University of Munich (TUM) RGB-D (Sturm et al. 2012) and Mobile Autonomous Robotic Systems lab (MARS) Mapper (Chen et al. 2020) systems should be mentioned. The former one features only the data from depth cameras and only a, MC GT trajectory (further extended by an IMU in a handheld system in the TUM VI dataset (Schubert et al. 2018)), while the latter contains data from multiple LiDAR devices, stereo camera and an IMU, as well as trajectory obtained with a tracking system and a TLS point cloud. In the scope of the ETH3D dataset (Schops et al. 2017), multiple image sequences obtained with a monocular camera and a stereo visual–inertial handheld system are shared. Most of them are recorded indoors, with a GT provided by a MC system. For a few scenes mapped outside, a GT is only reconstructed by a structure-from-motion (SfM) approach. From the most recent developments, interesting SLAM datasets start to include novel sensors such as event cameras (Klenk et al. 2021) and utilize simulation environments to facilitate the need for data acquisition in different conditions, especially for learning-based methods (Wang et al. 2020b). Nevertheless, the final evaluation of SLAM method performance should be assessed on real datasets, since multiple noise sources and possible failure factors present in the real world are extremely hard to reproduce in a simulated environment.

2.2 SLAM Datasets: Challenging Environments

All the above-mentioned datasets are, however, captured in relatively easy indoor, feature-rich environments. For mobile mapping underground sites, especially industrial facilities, conditions are much harder and include a multitude of potential noise sources, such as dust, variable humidity, uneven lighting, lack of distinct visual and geometrical features, vibrations, and uneven ground. These factors negatively affect possible assumptions in SLAM algorithm, e.g., the presence of planar features in the surveyed data. Dynamic conditions of the working machinery and possible rockfalls further contribute to the unpredictability of the environment and dangers that need to be recognized for a mobile robot working in such a facility. Thus, SLAM datasets acquired in such harsh conditions were investigated further: the HILTI

(Helmberger et al. 2022) and ConSLAM (Trzeciak et al. 2023) datasets from a construction site and the S3LI dataset (Giubilato et al. 2022) from Mount Etna in Italy, providing data of featureless, bare rock surface of the volcanic landscape. The HILTI dataset features multiple datasets from different editions, which vary in terms of the sensor suites used. Although the ConSLAM dataset provides data collected with a similar, prototypic sensor setup, it provides data from a periodically repeated measurements at the same construction site. Another challenging natural environment of a botanic garden was investigated by Liu et al. (2023), who share a dataset collected with a wheeled mobile robot with a rich sensor selection and a reliable ground truth 3D point cloud. A different challenging case could be considered for the mapping systems operating in areas with unreliable, partial GNSS signal coverage. An example of a dataset focusing on such conditions is BIMAGE Blaser et al. (2021), which provides raw data from a mobile mapping system collected in urban canyons and forest areas supplemented by ground control points surveyed with a total station.

The first underground SLAM dataset (Leung et al. 2017) was published in 2017 and featured data acquired in a Chilean underground mine recorded using a Clearpath UGV, equipped with a radar, stereo camera, and a Riegl TLS. The TLS was used in two ways: as a reference sensor, performing static scans when the robot was not moving, and similarly to an industrial-grade 3D LiDAR system, continuously scanning during robot's movement. However, utilizing such expensive instrument is not common, since it greatly increases the costs of the measurement system, is not suitable for flying units due to its weight, and the laser scan frequency is low (6 s for one full scan).

The most suitable datasets for evaluating robotic SLAM solutions for mining-related applications were acquired during the DARPA Subterranean (SubT) Challenge. Many teams shared data they collected during at least one of the events, which included a tunnel circuit, a power plant site and a cave system, all of which are relevant to the subject of our study. Datasets were published by the DARPA Army Research Lab (Rogers et al. 2020) and teams: Cerberus (Tranzatto et al. 2022), CoSTAR (Koval et al. 2022; Reinke et al. 2022), MARBLE (Kasper et al. 2019; Kramer et al. 2022), CTU-Cras-Norlab (Petracek et al. 2021; Krátký et al. 2021), Explorer (Wang et al. 2020a). They include UGV- and UAV-based data from stereo cameras, IMUs, and industrial-grade LiDAR scanners, seldom supplemented by thermal cameras and radars. The TLS-based GT was provided by DARPA. Although useful, those datasets usually feature expensive platforms (e.g., Boston Dynamics Spot) and do not have redundant sensors (multiple stereo cameras, LiDAR scanners, IMUs), making them solution dependent. A summary of the above-mentioned relevant open SLAM datasets is presented in Table 1.

Table 1 Comparison of selected relevant, popular SLAM open datasets

Dataset	Setting	LiDAR scanner		Camera		Inertial	Other sensors	GNSS	3D GT point cloud
		Spinning	Solid state	Stereo	RGB-D				
KITTI	Urban	✓	–	✓	✓	✓	–	✓	–
KAIST multispectral	Urban	✓	–	✓	–	✓	Thermal camera	✓	–
EuRoC	Indoor	–	–	✓	–	✓	–	–	✓
TUM VI	Indoor	–	–	✓	–	✓	–	–	–
ETH3D	Indoor and outdoor	–	–	✓	✓	✓	–	–	–
HILTI	Construction site	✓	✓	✓	–	✓	–	–	✓
ConSLAM	Construction site	✓	–	–	–	✓	Monocular and thermal cameras	–	✓
S3LI	Outdoor	–	✓	✓	–	✓	–	✓	–
Chilean underground mine	Underground	–	–	✓	–	–	TLS LiDAR, radar	–	✓
SubT: DARPA Army Research Lab	Underground	✓	–	✓	–	✓	–	–	✓
SubT: Cerberus	Underground	✓	–	✓	–	✓	–	–	✓
SubT: CoSTAR	Underground	✓	–	✓	✓	✓	Thermal camera, event camera, UWB beacons	–	–
SubT: MARBLE (ColoRadar)	Underground, indoor, and urban	✓	–	–	–	✓	Radars	–	–
SubT: CTU-Cras-Norlab	Underground	✓	–	✓	✓	✓	–	–	✓
MIN3D	Indoor and underground	✓	✓	✓	✓	✓	Thermal camera, multiple IMUs	–	✓

To move beyond a simple comparison between different SLAM algorithms (working on the data from the same sensor), we decided to enhance this approach, allowing to compare results from SLAM running on different sensors, acquired during the same sequence (e.g., solid-state and spinning LiDAR sensors, stereo and RGB-D camera). Moreover, utilizing low-cost solutions popular in the robotic community and sharing a survey-grade, TLS-based ground truth data, we allow researchers to evaluate SLAM software and hardware solutions that can be then used by them to create affordable systems for popularizing mobile mapping methods in underground applications.

3 The MIN3D Dataset

The data were collected in interior and exterior areas of the Wrocław University of Science and Technology (Fig. 1) and within some tunnels of the underground facility “Rzeczka”, which is a part of the “Riese” complex (Fig. 2), constructed during the World War II (Stach et al. 2014). Both sites feature varying surfaces and environments, which pose a challenge for SLAM algorithms as they must adapt to varying structural conditions, illumination changes, and the inconsistent level of the presence of distinct visual features.



Fig. 1 The employed multi-sensor UGV near the university building

3.1 Employed Robotic System and Sensor Configuration

The data were collected using a mobile robot equipped with a multi-sensory measuring column (Fig. 3). The robot was equipped with various sensors, as well as a data recording computer, power batteries, and lighting, which featured an adjustable intensity to adapt to the



Fig. 2 Mapped locations: underground tunnel (aka *adit*)

- An Intel RealSense D455 depth camera, placed below the Velodyne.
- Monocular RGB and IR cameras installed in the middle pair and featuring a similar optical system and field of view.
- A synchronized Basler stereo-rig.
- A Livox LiDAR scanner located at the bottom of the column.
- A NGIMU inertial measurement unit mounted at the robot base.

The data are supplemented by two IMU sensors integrated with an Intel RealSense camera and the Livox LiDAR system as well as an independent NGIMU. The robot was controlled manually from a remote operator panel. Control signals were transmitted in the 2.4 GHz frequency band, while data acquisition control telemetry was obtained from a tablet connected to a computer placed on the robot via a Wi-Fi network. The block diagram of the connected sensors is shown in Fig. 4, while the remote visualization and control

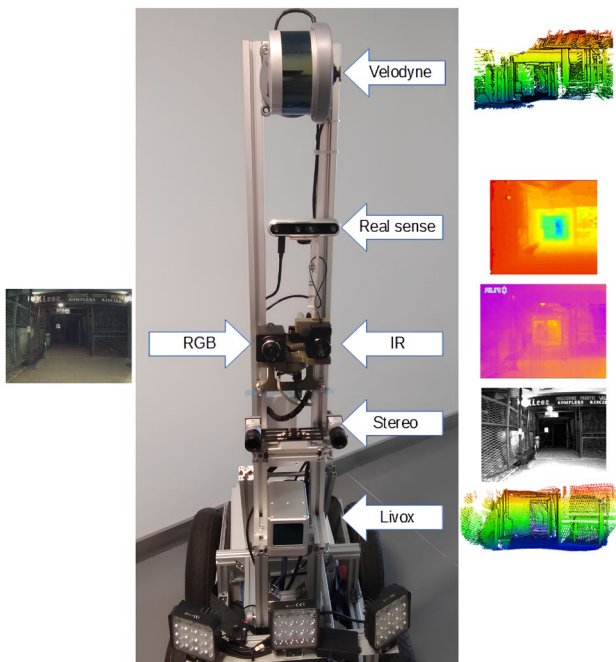


Fig. 3 The mobile robot with its sensors placed along the vertical column bar with the example data frames (adapted from: Trybała et al. 2022)

environmental conditions and enable the recording of image data in low-light environments. The list of utilized devices includes:

- A Velodyne LiDAR scanner, mounted at the top of the measuring column through an additional rotation module, which increases the resolution of the acquired data by rotating the sensor around the horizontal axis.

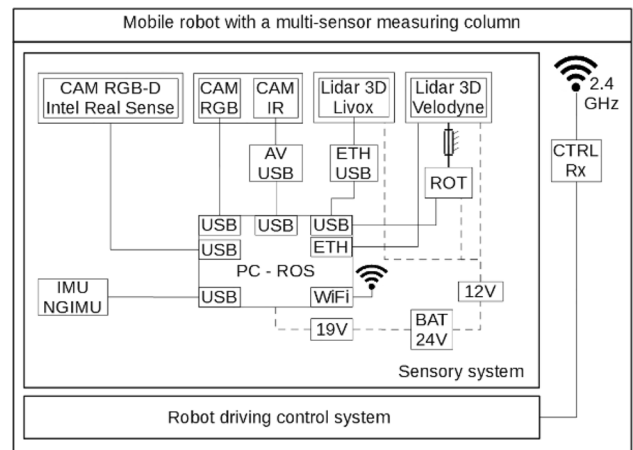


Fig. 4 Block diagram of a robotic multi-sensory measurement system (Trybała et al. 2022)

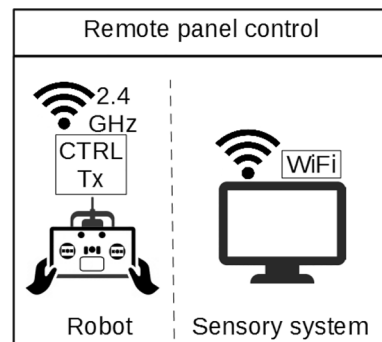


Fig. 5 Remote visualization and control panel (Trybała et al. 2022)

Table 2 Characteristics of the acquired data

Sequence	Path sketch	Size/length	Data acquisition aim	Data samples	Total size
University 1: ground level ^a	Figure 6	60 m × 40 m /220 m	Whole area mapping, longer route, reflective surfaces, lack of visual features	53,147 images 10,163 point clouds 130,370 IMU readings	26.1 GB
University 2: indoor/outdoor	Figure 7	50 m × 20 m/120 m	Indoor/outdoor transition with changing illumination	26,419 images 5359 point clouds 111,500 readings	22.1 GB
University 3: lab loop closures	Figure 8	20 m × 10 m/90 m	Changing illumination in different rooms, multiple loop closures	25,519 images 5093 point clouds 159,215 IMU readings	18.9 GB
Tunnel 1: forward pass ^b	Figure 9	80 m × 5 m/80 m	Basic bare rock tunnel mapping, sparse geometrical and visual features	22,244 images 5785 point clouds 180,813 IMU readings	13.2 GB
Tunnel 2: return pass ^b	Figure 10	80 m × 5 m/80 m	Basic bare rock tunnel mapping, sparse geometrical and visual features. Possibility of multi-session mapping with previous dataset	19,104 images 4156 point clouds 129,952 IMU readings	10.8 GB
Tunnel 3: main tunnel with loops, part 1 ^b	Figure 11	70 m × 20 m/120 m	Loop closures in underground conditions, transitions between unstructured/structured geometry	27,198 images 7074 point clouds 221,094 IMU readings	17.9 GB
Tunnel 4: main tunnel with loops, part 2 ^{b,c}	Figure 11	40 m × 20 m/60 m	Loop closures in underground conditions, transitions between unstructured/structured geometry. Kidnapped robot problem if analyzed jointly with previous dataset	12,821 images 3336 point clouds 37,303 IMU readings	13.9 GB
Tunnel 5: secondary tunnel ^{b,c}	Figure 12	90 m × 10 m/100 m	Basic bare rock tunnel mapping, transitions between unstructured/structured geometry	19,884 images 5172 point clouds 57,828 IMU readings	22.5 GB

^aVelodyne LiDAR sensor placed horizontally

^bBasler stereo with limited frame rate

^cNo RealSense IMU data

panel are shown in Fig. 5. A methodology for system calibration, i.e., estimation of the relative orientation between sensors, was presented in Trybała et al. (2022).

3.2 Data Acquisition

A total of eight datasets were acquired in two different settings:

- Three sequences inside and around the research building of the Faculty of Geoengineering, Mining and Geology at Wrocław University of Science and Technology (Poland).
- Five sequences in the underground site “Rzeczką”, part of the “Riese” underground complex (Walim, Poland).

The conditions of the university dataset resemble an industrial environment, with mostly monochromatic colors, scarce visual features, long and uniform corridors, and the presence of reflective surfaces. During the acquisitions in the subterranean environment, the robot was equipped with its own lighting system due to the absence of illumination

in a huge part of the mine. These real underground conditions allowed to illustrate the challenges often encountered in a setting of an industrial mine, where irregular tunnels carved or blasted in rock are mixed with reinforced, more structured areas.

To further increase the level of difficulty for SLAM algorithms, the acquisitions featured illumination changes (robot driving from indoor to outdoor or through a room with light turned off) and frequent revisiting of the same area, often from different perspectives. The specific aims of each acquisition, together with resulting data size, has been summed up in Table 2. Approximate robot trajectories for each sequence, drawn on a 2D projection of the ground truth point cloud cross sections, are shown in Figs. 6, 7, 8, 9, 10, 11, 12.

Due to some problems with the reliability of RealSense internal IMU, an additional NGIMU sensor was added to the measurement system. However, we still provide the incomplete data from the RealSense device, since it may allow some interesting analyses and development in terms of multi-IMU systems, as discussed further in Sect. 4. Similarly, probably due to the challenging environmental

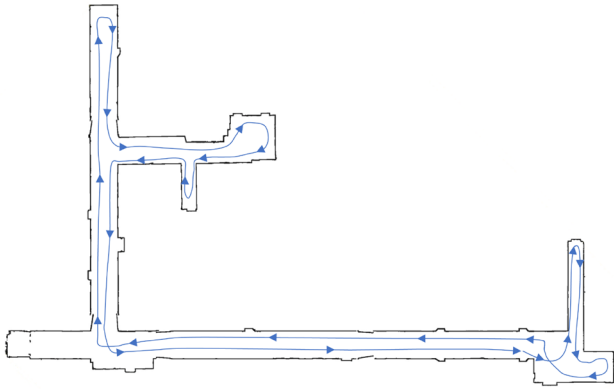


Fig. 6 Sketch of the robot trajectory in the university building (Sequence University 1): textureless ground floor

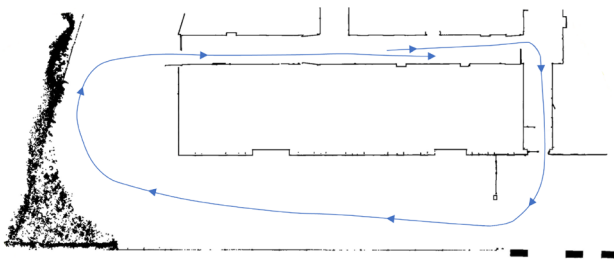


Fig. 7 Sketch of the robot trajectory in the university building (Sequence University 2): indoor–outdoor transitions

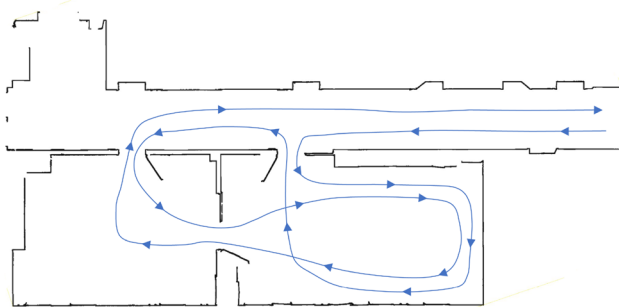


Fig. 8 Sketch of the robot trajectory in the university building (Sequence University 3): ground floor (Sequence 1)

conditions, the Basler stereo camera rig was not able to maintain the desired frame rate during the tunnel tests. Direct processing of this data will result in worse results than for images from other cameras, but might facilitate the development and evaluation of, e.g., AI-based image denoising and frame rate interpolation methods for robustifying mobile robotic applications in challenging environments.

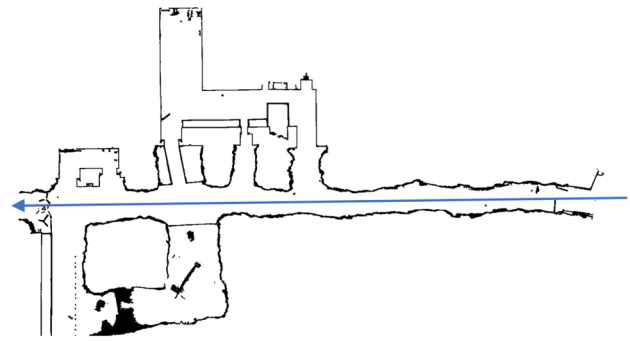


Fig. 9 Sketch of the robot trajectories in the underground tunnel (Sequence Underground 1): main tunnel, forward pass

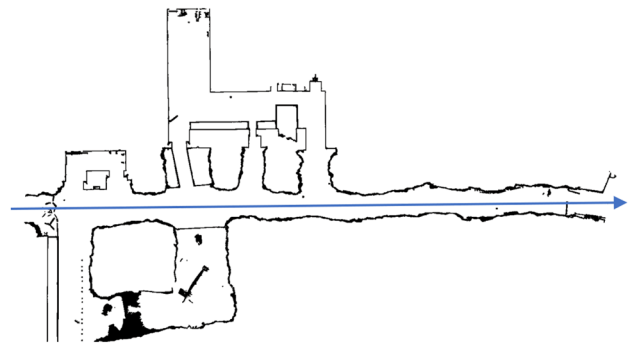


Fig. 10 Sketch of the robot trajectories in the underground tunnel (Sequence Underground 2): main tunnel, return pass

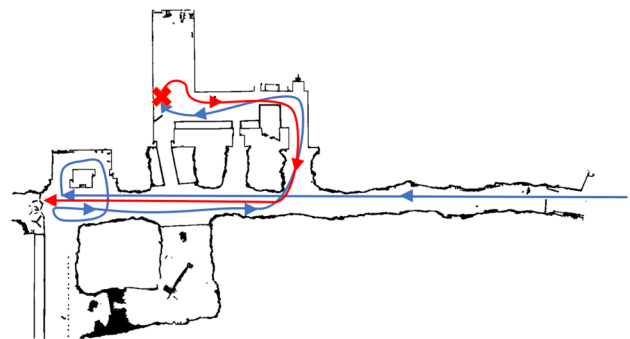


Fig. 11 Sketch of the robot trajectories in the underground tunnel (Sequences Underground 3 & 4): pass with multiple loops. Route is split into two sequences: before (blue) and after (red) kidnapping a robot (position marked as a red cross)

3.3 Dataset Structure

The data were recorded using an Intel NUC machine and, during the measurements, saved in the .rosbag file format using ROS (Robot Operating System) Melodic (Quigley et al. 2009) and common driver packages. In the post-processing operations, the data were unpacked and converted

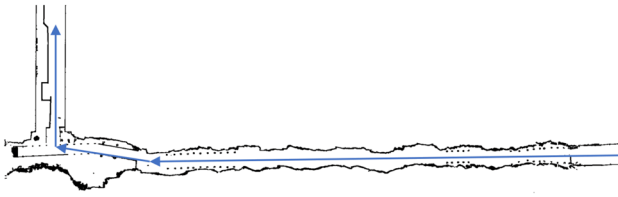


Fig. 12 Sketch of the robot trajectories in the underground tunnel (Sequence Underground 5): secondary tunnel

to open formats suitable for further analyses, as shown in Table 3.

The naming convention of the files is $\langle ROS\ timestamp \rangle \langle dot \rangle \langle extension \rangle$, since all data were time-stamped in a centralized manner, according to the ROS master node clock. However, time stamps of some of the data were already pre-synchronized by the respective device drivers. Time stamps for: RealSense RGB, IR images, depth maps, and IMU are synchronized to each other, as well as

Table 3 Data types and file formats

Source of data	Type of data	File format
Velodyne LiDAR scanner	Point cloud	.ply
Livox LiDAR scanner	Point cloud	.ply
RGB camera	Image	.png
FLIR IR camera	Image	.png
RealSense RGB camera	Image	.png
RealSense stereo IR camera	Images	.png
RealSense precomputed depth map	Image	.png
Basler stereo camera	Images	.png
IMU Livox	Linear acceleration, angular velocity	.csv
IMU RealSense	Linear acceleration, angular velocity	.csv
IMU NGIMU	Linear acceleration, angular velocity	.csv

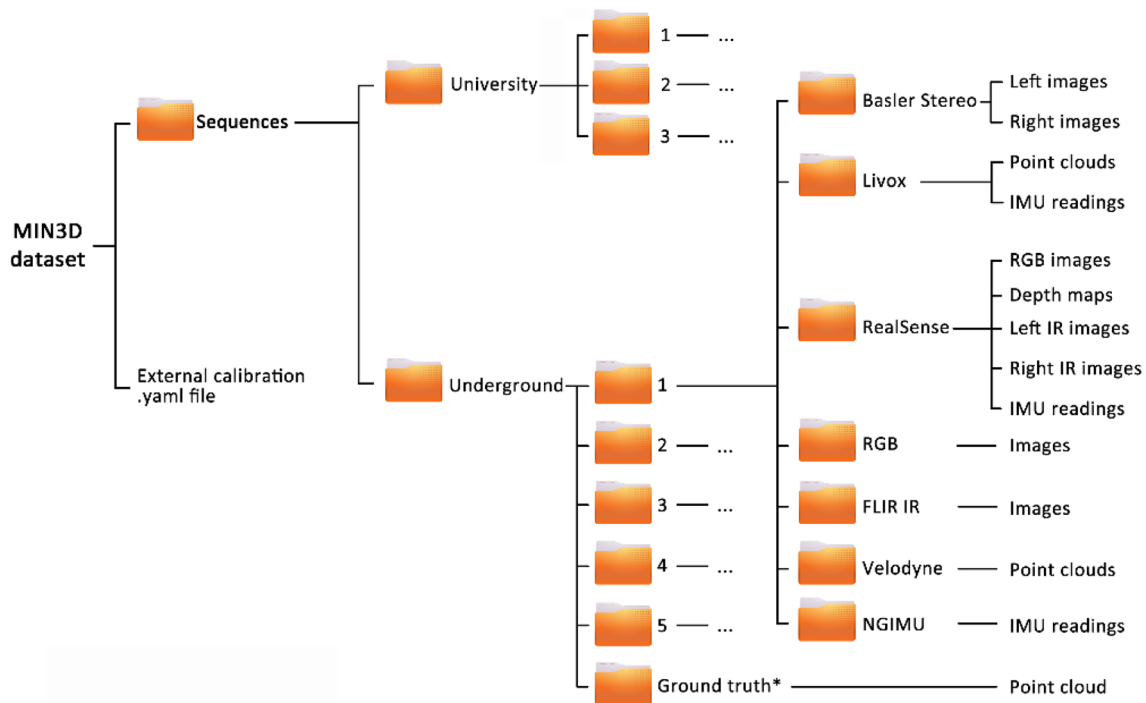


Fig. 13 File structure of the MIN3D dataset. Separate ground truth point clouds are provided for each of the three university sequences, but a single reference point cloud is shared for all five sequences of the underground facility

Basler stereo pairs and Livox point clouds with its internal IMU. The dataset general structure is explained in Fig. 13.

3.4 Ground Truth and Evaluation Methodology

Reference data were acquired using a RIEGL VZ-400i terrestrial laser scanner (Fig. 14). The scanner features a laser pulse repetition rate of 100–1200 kHz, a maximum effective measurement rate of 500,000 points/s, and a measurement range of 0.5 m to 800 m. The scanning angle range is a total of 100° in a vertical line and max. 360° in the horizontal frame. The manufacturer's stated accuracy of resulting single point 3D position is 5 mm and the declared precision is 3 mm (Riegl datasheet 2019).

For both test sites, the distance between consecutive scan positions was about 5–15 m. The scanning parameters used were a laser pulse repetition rate of 1200 kHz, a scanning resolution of 0.05°, and a point cloud resolution characterized by point-to-point distance of 17.5 mm at a distance of 20 m.

The processing of the acquired TLS data was carried out in the dedicated RiSCAN PRO software (RIEGL Laser Measurement Systems GmbH 2019) for point cloud filtering and scan registration. The preliminary scan registration was performed using an automatic registration method based on voxels extraction and fitting. To improve scan position registration, alignment was performed using the multi station adjustment (MSA) procedure. The position and orientation of each scan position were adjusted in a bundle adjustment (BA), which included several iterations to minimize position error between overlapping planes and determine the best fit.

The alignment process resulted in an error (i.e., scanner position standard deviation after BA) of ca 2 mm for both test sites. Control of the alignment of the overlapping first and last positions, creating a loop, showed a spatial matching within 5 mm. This quality control was omitted only for the GT point cloud of the first university sequence, which does not include a loop. The resulting point cloud of the building test site and the underground facility are shown in Figs. 15 and 16, respectively.

To facilitate the proper matching of measurement data with GT, reference points in the form of white spheres with a diameter of 100 mm were placed in the area of interest of both test sites (Fig. 17). The reference targets were selected to be properly visible by all the optical sensors mounted on the robot.

4 Processing and Analyses

The MIN3D dataset could support evaluations of 3D mapping methods, including SLAM. As multiple approaches to assess the quality of the mapping results exist, we do not provide a dedicated benchmarking tool and leave the decision of selecting an appropriate workflow to the readers. Pipelines developed for ETH3D (Schops et al. 2017), 3D Tanks and Temples (Knapitsch et al. 2017), as well as a more sophisticated analysis presented by Toschi et al. (2015) could be mentioned as examples of sound methodologies for carrying out quality evaluation of the 3D reconstruction for the results achieved from processing MIN3D data.

An overview of current state-of-the-art strategies of tackling common problems, based on the research and experiences from the DARPA Subterranean Challenge, in applying SLAM in underground environments can be found in Ebadi et al. (2022). Moreover, we also envision a MIN3D contribution toward the development of specific algorithms for challenging mining environments (Fig. 18), which includes, e.g., dedicated methods for dealing with various structuration levels of geometry, loop closure detection in mostly featureless conditions, or point cloud filtering and optimization approaches.

4.1 Underground Mobile Mapping Accuracy

During the preliminary evaluation of SLAM on our dataset, comparisons of the point clouds obtained with example SLAM algorithms were carried out on representative sequences of the dataset. One sequence has been selected from the indoor part of the dataset (University 2) and two sequences were chosen from the underground tunnels (Underground 1 and 3). Based on the state-of-the-art research, we chose one V-SLAM algorithm, one LiDAR-inertial algorithm, and one pure-LiDAR method. We processed:

- RealSense RGB-D data with ORB-SLAM3 (Campos et al. 2021).
- Livox LiDAR scanner and IMU data with FAST-LIO SLAM (Kim et al. 2021; Xu et al. 2022).
- Actuated Velodyne LiDAR scanner data with SC-A-LOAM (Kim et al. 2022).

As representative statistics, summarizing the mapping performance of each of those methods, we have chosen mean, standard deviation, and $(-3\sigma, 3\sigma)$ range of cloud-to-cloud distance distributions, calculated as signed distances using M3C2 plugin of Cloud Compare software (Lague et al. 2013).



Fig. 14 RIEGL VZ-400i terrestrial laser scanner

Point clouds based on the simultaneously acquired data from three different sensors were obtained using the previously mentioned state-of-the-art mobile mapping methods. They were then registered to the GT model using iterative closest point (ICP; Besl and McKay 1992) with an initial manual alignment. Mapping errors were estimated as the distances between the point clouds and the local GT model and signed according to their estimated normals. The error distributions were analyzed together with the qualitative analysis of the results (long- and short-term drifts, topology correctness). Summary statistics of the quantitative analysis of the mapping error distributions are presented in Table 4.

Fig. 16 Top view of reference TLS point clouds with the locations of the scan positions (in red): tunnels of the underground area. Part of the point cloud, representing the outdoor area irrelevant for the dataset, is not displayed

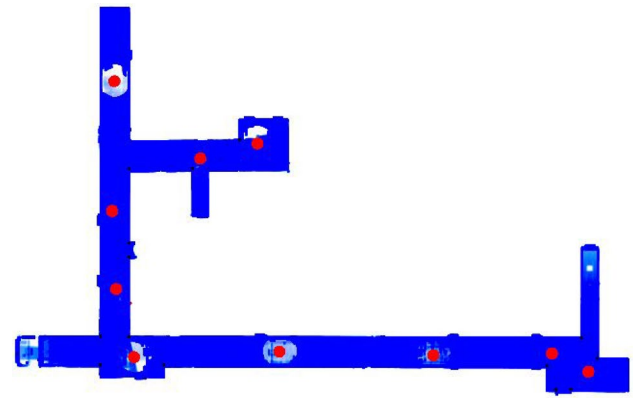
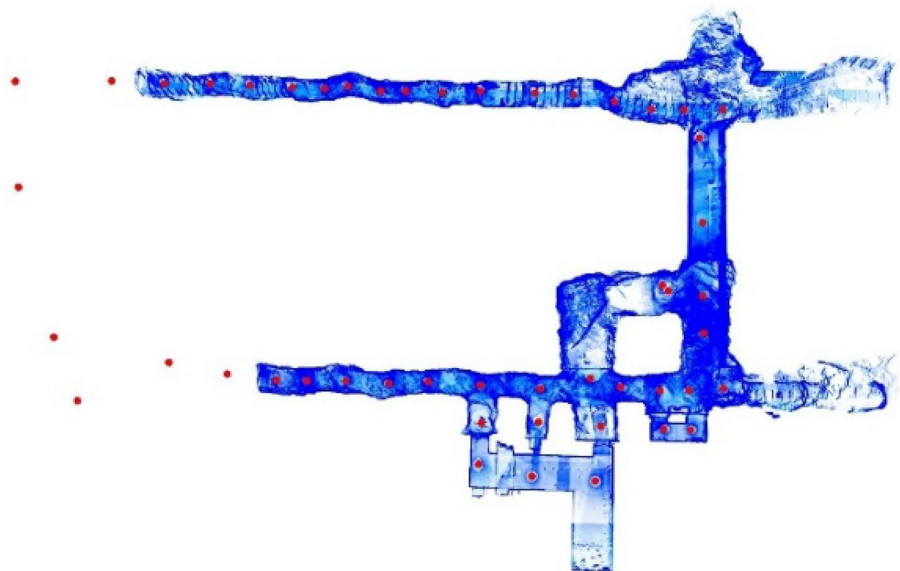


Fig. 15 Top view of reference TLS point clouds with the locations of the scan positions (in red): university ground floor, sequence 1

The obtained results show that the tested methods were appropriate for 3D mapping of the examined areas. Using a common color-coding scheme (Fig. 19), we compare the results of accuracy evaluation of the three tested SLAM approaches (Figs. 20, 21, 22). Qualitatively analyzing them, the resulting point clouds present the “correct” topology comparing to the GT data. However, in-depth analysis often revealed inconsistencies such as lack of proper loop closures, high short-term rotational drifts, long-term rotational drift around the robot’s roll axis, and increased noise near reflective surfaces. Those resulted in point cloud errors such as “ghosting”, i.e., not-aligned point clouds of areas measured multiple times or dimension deformation, i.e., shortening of the tunnel length. The above-mentioned issues occurred in both indoor and underground datasets and their example visualizations are presented in Fig. 23. It is worth mentioning



Fig. 17 References object on robot path in the building corridor (left) and in the underground tunnel area (right)

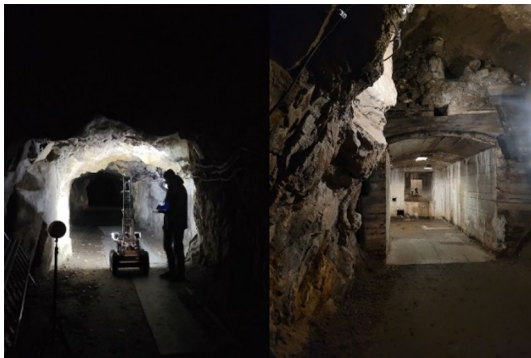


Fig. 18 Challenges for SLAM in the underground environment: uneven illumination, lack of visual features (left); changing types of geometry: passage from an unstructured tunnel to a concrete corridor (right)

that no algorithm was able to properly recover from the simulation of the kidnapped robot problem between sequences Underground 3 and 4 using loop closure detection. Thus, Underground 3 was analyzed only as a standalone sequence.

4.2 Multi-sensor Signal Analysis

Apart from the core issue of improving robustness and reliability of various mobile mapping and localization

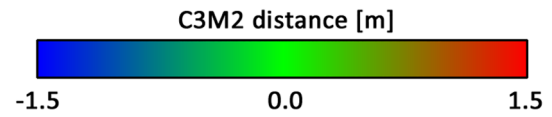


Fig. 19 Universal color scale used in all point cloud visualizations in Figs. 20, 21, 22, and 23

approaches, we encourage using the proposed MIN3D dataset also for other purposes, such as image enhancement. Conditions in which the data were acquired can challenge state-of-the-art image processing methods. Such methods include, but are not limited to, image deblurring and upscaling, frame interpolation, depth estimation from monocular camera (or improving the quality of depth obtained with the stereo images), and application of different 3D geometry reconstruction methods. Evaluations of deep learning-based techniques are foreseen, since scarcity of the training data from unique, underground conditions may seriously hinder their performance on the MIN3D dataset.

Furthermore, simultaneous acquisition of data from various sensors allows exploration of novel data fusion methods: this could also include methods for improving the quality of the data using multiple devices. As an example, we show a proof of concept of utilizing two IMUs in the context of possible developments in the area of the positioning methods using multiple inertial devices. We compared signals from IMUs installed in Livox and RealSense, with the focus on acceleration data. Figure 24 presents raw data from the sensors expressed in g units.

Firstly, the moving average of the absolute value of the signals was calculated for every channel with the window of 1 s (see Fig. 25). This way, an average variability of vibration strength can be visualized and compared per axis. The main visible difference between devices is expressed as slightly stronger vibrations in the horizontal plane for RealSense compared to Livox. It can be explained by the fact that RealSense was mounted higher on the sensor column, and angular movements of the entire column, with respect

Table 4 Statistics of the mapping error distributions for selected SLAM algorithms

Dataset	Mean mapping error [cm]			Standard deviation [cm]			95% of mapping error distribution range [m]		
	ORB-SLAM3	FAST-LIO-SLAM	SC-A-LOAM	ORB-SLAM3	FAST-LIO-SLAM	SC-A-LOAM	ORB-SLAM3	FAST-LIO-SLAM	SC-A-LOAM
University 2	− 3.5	2.8	− 7.7	101	31	54	(− 2.20, 1.72)	(− 0.65, 0.38)	(− 1.29, 0.85)
Underground 1	− 3.8	0.7	− 8.9	47	23	60	(− 1.26, 0.41)	(− 0.11, 0.14)	(− 1.63, 0.73)
Underground 3	− 3.5	2.5	− 14.6	45	16	81	(− 1.33, 0.46)	(− 0.15, 0.29)	(− 2.30, 1.44)

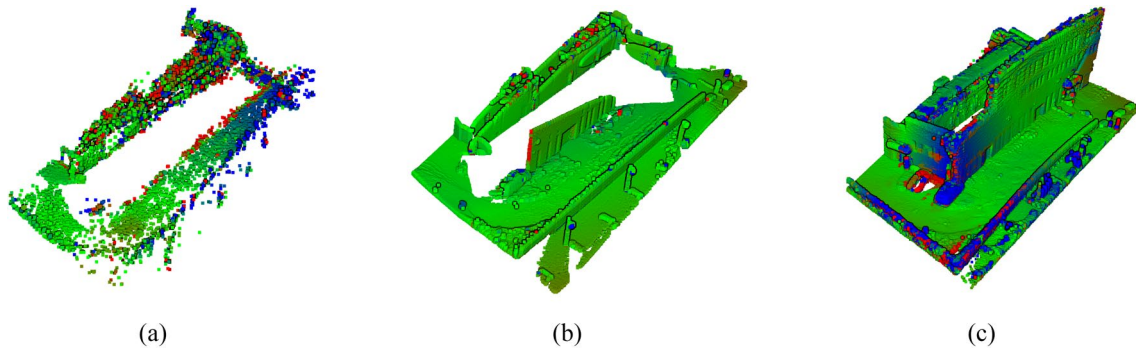


Fig. 20 Examples of SLAM results on the University 2 sequence: **a** ORB-SLAM3 (sparse point cloud); **b** FAST-LIO-SLAM; **c** SC-A-LOAM

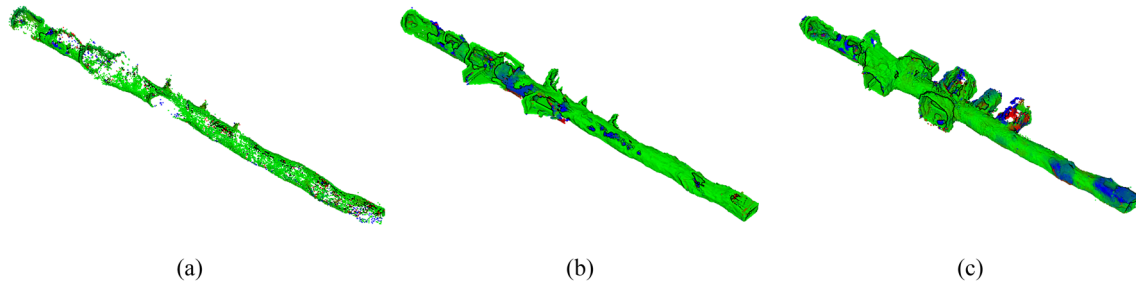


Fig. 21 Examples of SLAM results on the Underground 1 sequence: **a** ORB-SLAM3 (sparse point cloud); **b** FAST-LIO-SLAM; **c** SC-A-LOAM

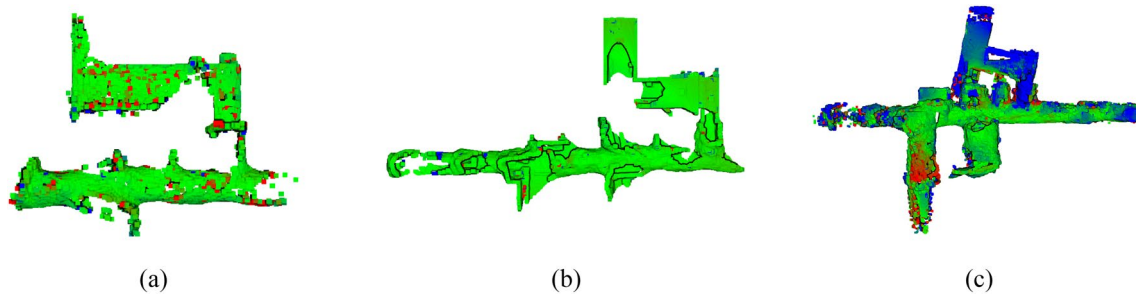


Fig. 22 Examples of SLAM results on the Underground 3 sequence: **a** ORB-SLAM3 (incomplete sparse point cloud); **b** FAST-LIO-SLAM; **c** SC-A-LOAM

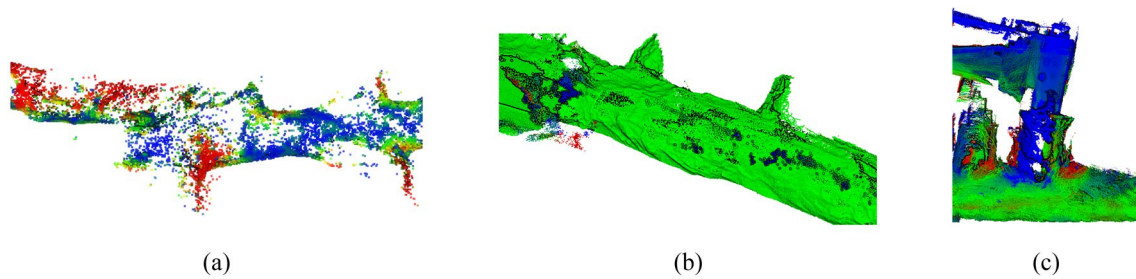


Fig. 23 Issues in various SLAM results: **a** large linear drift error at the straight start of Underground 2 dataset (ORB-SLAM3); **b** double wall error and noisy points in the Underground 1 dataset (FAST-LIO-SLAM); **c** angular drift at the end of Underground 3 dataset (SC-A-LOAM)

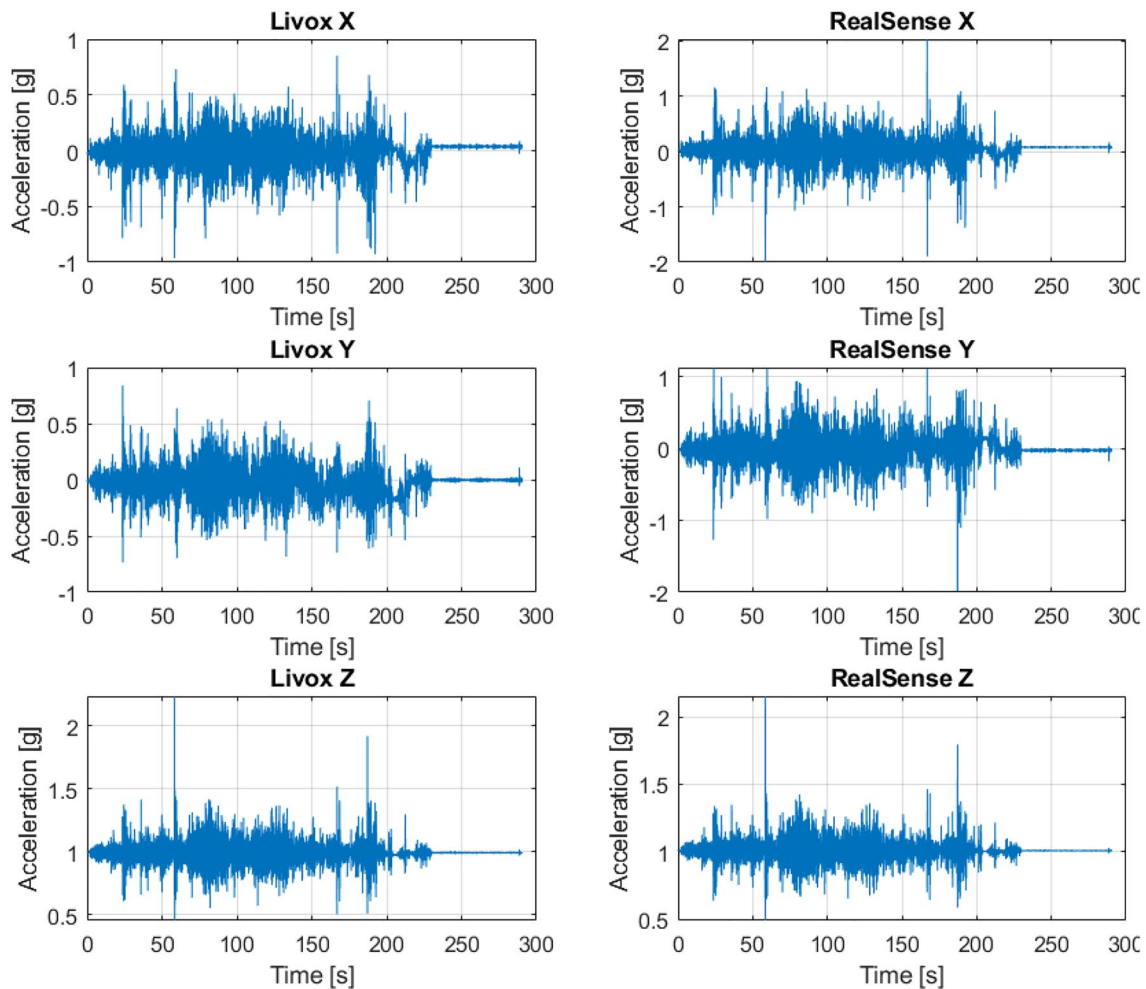


Fig. 24 Raw signals from IMU accelerometers of Livox and RealSense

to the pivot point at the bottom of the column, translate to stronger readings of the RealSense IMU.

In the second step, a moving variance was calculated for all channels, also with the window length of 1 s (see Fig. 26). Comparison of vibrations in the XY directions shows that there is a visible proportional relation between the energy of vibration of each device. It could be explained by the fact that the devices are mounted at different heights on the column, and the angular nature of the vibrations of the column causes the amplification of vibrations in the lateral plane as a function of the height of the column.

The authors attempted to evaluate the relation between vibration energy for the devices. The best achieved fit was a linear model with the ratio of 2.93 at $R^2=0.91$ (Fig. 27). It shows that RealSense at its mounting point experiences almost $3 \times$ more energetic vibration in the horizontal plane in relation to Livox due to the angular vibrations of the column. Additionally, the linear nature of the model, as

well as the coefficient of 2.93 can be confirmed by the fact that Livox is mounted 30 cm above the pivot point (bottom mount of the column) and RealSense is placed at 88 cm above the pivot point, which is 2.933 times higher.

5 Conclusions

The paper presented a novel UGV-based dataset for developing and testing mobile mapping solutions (e.g., SLAM) in challenging GNSS-denied conditions, common in mining applications or textureless indoor spaces. We provide data sequences collected simultaneously with multiple sensors, including different LiDAR scanners, cameras, and inertial units. The environments of tests were selected to pose a challenge for state-of-the-art data processing algorithms and feature changing illumination, varying complexity of geometry, and textureless areas. Acquisitions were carried out inside a university building and in an underground historical tunnel,

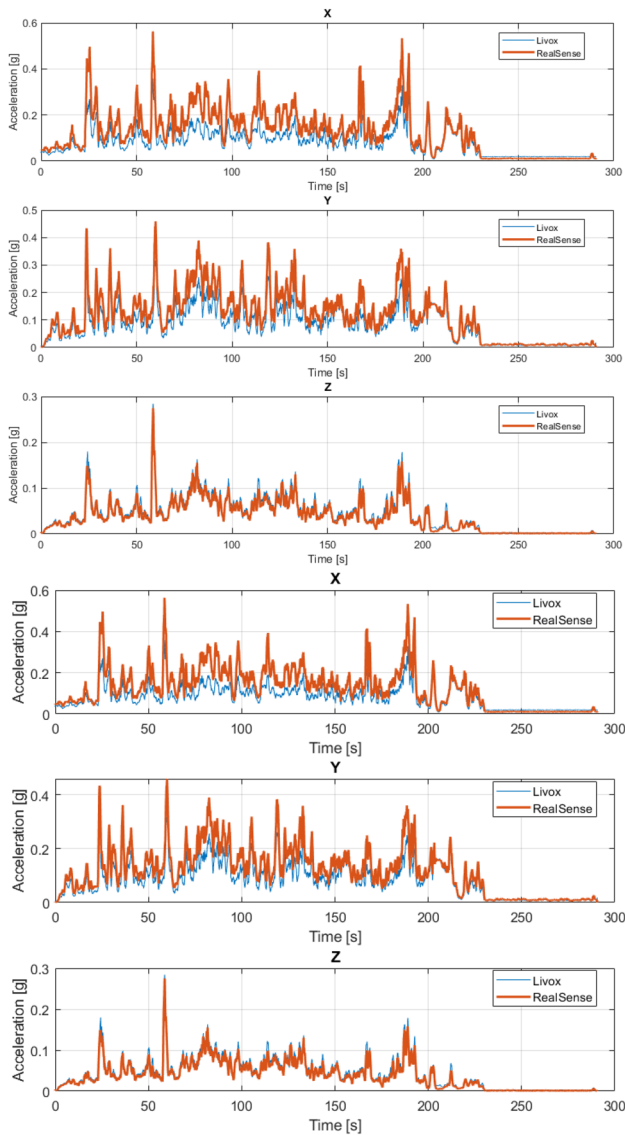


Fig. 25 Moving average of absolute values for all axes with the window of 1 s. Axes X and Y (vibrations on the horizontal plane) show stronger vibration for RealSense, which was mounted higher on the column

which allows to also evaluate the performance degradation of developed methods between real and simulated conditions. Such analysis would be especially valuable for learning-based approaches.

We presented quantitative evaluations of selected SLAM methods utilizing data from different sensors (cameras, LiDAR devices, IMU) and showed some shortcomings in their performance when applied to the MIN3D data. Additionally, an analysis of data from the multi-IMU system was performed to showcase the possible directions of research of multi-sensor data fusion.

In summary, it is envisaged that the utilization of the MIN3D dataset has the potential to accelerate

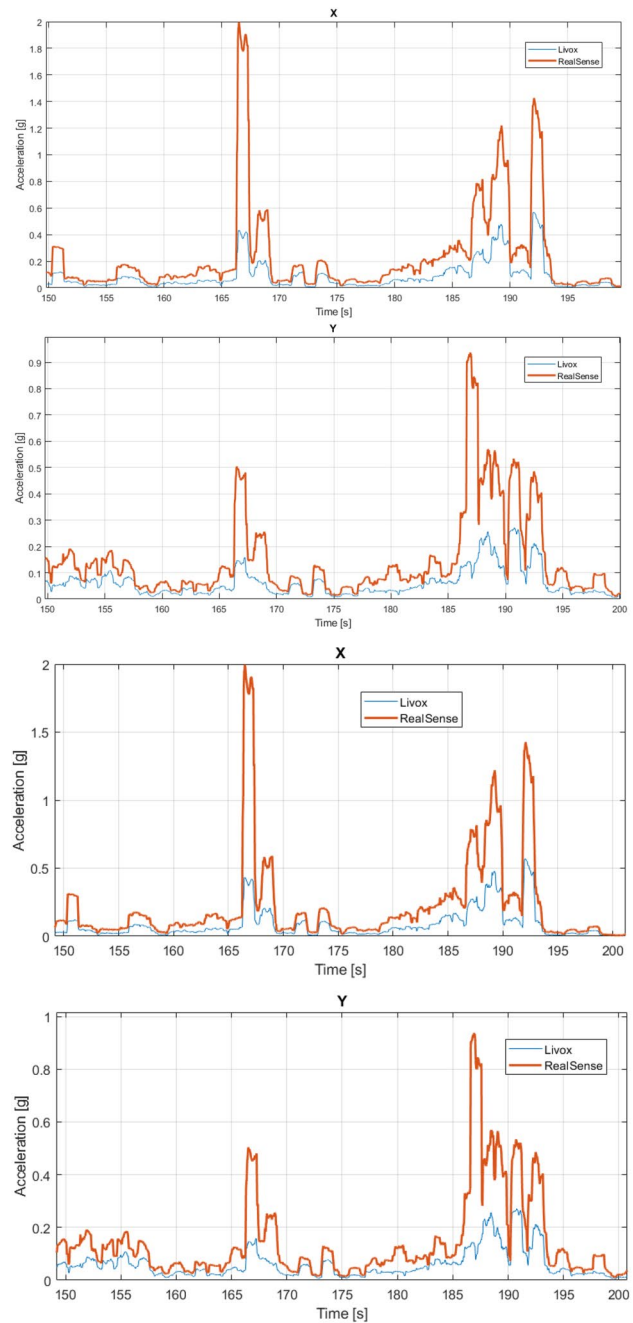


Fig. 26 Moving variance for IMU linear accelerations X and Y (comparison per axis) with a window of 1 s. Significant proportional relation between vibration energy is revealed, which is a result of height difference of the mounting points on the column

advancements in multiple research domains within the field of robotics, computer vision and geomatics, acknowledging that the list provided below is not exhaustive:

- Testing and improving mapping approaches (visual, LiDAR, fusion) in the challenging underground or indoor conditions.

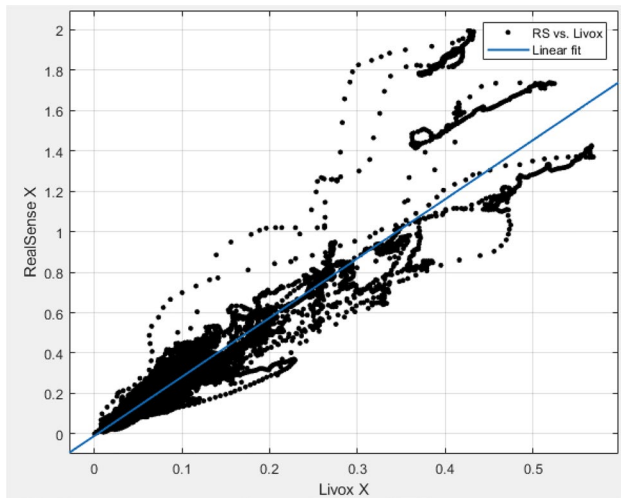


Fig. 27 Relation between vibration energy of the devices evaluated based on the X axis of IMU linear acceleration

- Robustifying V-SLAM in the environments with changing illumination.
- Estimating depth with a monocular camera.
- Developing visual and LiDAR-based loop closure detection algorithms in degraded environments.
- Using multi-sensor odometry and mapping approaches (multi-IMU, multi-camera, multi-LiDAR).
- Online calibration and utilization of multi-sensor suites, including cameras with different spectral responses (e.g., RGB and thermal).

Acknowledgements The authors offer special thanks to Walimskie Drifts in Walim (<https://sztolnie.pl>) for making the facility available for data acquisition.

Author Contributions Conceptualization, PT, JS, JW and FR; methodology, PT, JS, FR; software, PT; validation, PT, JS, JW and PK; investigation, PT, JS, JW and PK; resources, FR, JB and RZ; data curation, PT, JS and JW; writing—original draft preparation, PT, JS; writing—review and editing, PK, JW, FR, JB and RZ; visualization, PT, PK and JW; supervision, FR, JB and RZ; project administration, FR, JB and RZ; funding acquisition, FR, JB and RZ. All authors have read and agreed to the published version of the manuscript.

Funding This work was partly supported by EIT RawMaterials GmbH within the activities of the AMICOS—Autonomous Monitoring and Control System for Mining Plants—project (Agreement No. 19018) and VOT3D—project (Agreement No. 21119). The work was also partly supported by the FAIR project, Piano Nazionale di Ripresa e Resilienza.

Data Availability Datasets have been published at <https://3dom.fbk.eu/benchmarks>.

Declarations

Conflict of Interest The authors declare no conflict of interest.

Open Access This article is licensed under a Creative Commons Attribution 4.0 International License, which permits use, sharing, adaptation, distribution and reproduction in any medium or format, as long as you give appropriate credit to the original author(s) and the source, provide a link to the Creative Commons licence, and indicate if changes were made. The images or other third party material in this article are included in the article's Creative Commons licence, unless indicated otherwise in a credit line to the material. If material is not included in the article's Creative Commons licence and your intended use is not permitted by statutory regulation or exceeds the permitted use, you will need to obtain permission directly from the copyright holder. To view a copy of this licence, visit <http://creativecommons.org/licenses/by/4.0/>.

References

- Besl PJ, McKay ND (1992) Method for registration of 3-D shapes. In: Sensor fusion IV: control paradigms and data structures. pp 586–606
- Blanco-Claraco J-L, Moreno-Duenas F-A, González-Jiménez J (2014) The Málaga urban dataset: high-rate stereo and LiDAR in a realistic urban scenario. *Int J Rob Res* 33:207–214
- Blaser S, Nebiker S, Wisler D (2019) Portable image-based high performance mobile mapping system in underground environments—system configuration and performance evaluation. *ISPRS Ann Photogramm Remote Sens Spatial Inform Sci* 4:255–262
- Blaser S, Meyer J, Nebiker S (2021) Open urban and forest datasets from a high-performance mobile mapping backpack—a contribution for advancing the creation of digital city twins. *Int Arch Photogramm Remote Sens Spat Inf Sci* 43:125–131
- Burri M, Nikolic J, Gohl P, Schneider T, Rehder J, Omari S, Achtelik MW, Siegwart R (2016) The EuRoC micro aerial vehicle datasets. *Int J Rob Res* 35:1157–1163
- Campos C, Elvira R, Rodriguez JGG, Montiel JMM, Tardós JD (2021) Orb-slam3: an accurate open-source library for visual, visual-inertial, and multimap slam. *IEEE Trans Rob* 37:1874–1890
- Chen H, Yang Z, Zhao X, Weng G, Wan H, Luo J, Ye X, Zhao Z, He Z, Shen Y, Schwertfeger S (2020) Advanced mapping robot and high-resolution dataset. *Rob Auton Syst* 131:103559
- Chiang KW, Tsai G-J, Zeng JC (2021) *Mobile mapping technologies*. Springer
- Choi Y, Kim N, Hwang S, Kibaek P, Yoon JS, An K, Kweon IS (2018) KAIST multi-spectral day/night data set for autonomous and assisted driving. *IEEE Trans Intell Transp Syst* 19:934–948
- Chung TH, Orekhov V, Maio A (2023) Into the robotic depths: analysis and insights from the DARPA subterranean challenge. *Annu Rev Control Robot Auton Syst* 6:477–502
- Cordts M, Omran M, Ramos S, Scharwächter T, Enzweiler M, Benenson R, Franke U, Roth S, Schiele B (2015) The Cityscapes Dataset. In: *CVPR Workshop on The Future of Datasets in Vision*
- Dabek P, Szrek J, Zimroz R, Wodecki J (2022) An automatic procedure for overheated idler detection in belt conveyors using fusion of infrared and RGB images acquired during UGV robot inspection. *Energies* 15:601. <https://doi.org/10.3390/en15020601>
- Di Stefano F, Torresani A, Farella EM, Pierdicca R, Menna F, Remondino F (2021) 3D surveying of underground built heritage: opportunities and challenges of mobile technologies. *Sustainability* 13:13289
- Ebadi K, Bernreiter L, Biggie H, Catt G, Chang Y, Chatterjee A, Deniston CE, Deschênes S-P, Harlow K, Khattak S, Nogueira L, Palieri M, Petráček P, Petrлік M, Reinke A, Krátký V, Zhao S, Agha-mohammadi A, Alexis K, Carlone L (2022) Present and future of slam in extreme underground environments. *arXiv preprint arXiv:220801787*

- Elhashash M, Albanwan H, Qin R (2022) A review of mobile mapping systems: from sensors to applications. *Sensors* 22:4262
- Feng Y, Xiao Q, Brenner C, Peche A, Yang J, Feuerhake U, Sester M (2022) Determination of building flood risk maps from LiDAR mobile mapping data. *Comput Environ Urban Syst* 93:101759. <https://doi.org/10.1016/j.compenvurbysys.2022.101759>
- Funk N, Tarrío J, Papatheodorou S, Popović M, Alcantarilla PF, Leutenegger S (2021) Multi-resolution 3D mapping with explicit free space representation for fast and accurate mobile robot motion planning. *IEEE Robot Autom Lett* 6:3553–3560
- Geiger A, Lenz P, Urtasun R (2012) Are we ready for autonomous driving? The KITTI vision benchmark suite. In: 2012 IEEE Conference on Computer Vision and Pattern Recognition. IEEE
- Geiger A, Lenz P, Stiller C, Urtasun R (2013) Vision meets robotics: the KITTI dataset. *Int J Rob Res* 32:1231–1237
- Giubilato R, Sturzl W, Wedler A, Triebel R (2022) Challenges of SLAM in extremely unstructured environments: the DLR planetary stereo, solid-state LiDAR, inertial dataset. *IEEE Robot Autom Lett* 7:8721–8728
- Helmberger M, Morin K, Berner B, Kumar N, Cioffi G, Scaramuzza D (2022) The Hilti SLAM challenge dataset. *IEEE Robot Autom Lett* 7:7518–7525
- Huang A, Antone M, Olson E, Fletcher L, Moore D, Teller S, Leonard J (2010) A high-rate, heterogeneous data set from the Darpa urban challenge. *Int J Robot Res* 29:1595–1601. <https://doi.org/10.1177/0278364910384295>
- Jeong J, Cho Y, Shin Y-S, Roh H, Kim A (2019) Complex urban dataset with multi-level sensors from highly diverse urban environments. *Int J Rob Res* 38:642–657
- Kanellakis C, Nikolakopoulos G (2016) Evaluation of visual localization systems in underground mining. In: 2016 24th Mediterranean Conference on Control and Automation (MED). pp 539–544
- Kasper M, McGuire S, Heckman C (2019) A benchmark for visual-inertial odometry systems employing onboard illumination. In: 2019 IEEE/RSJ International Conference on Intelligent Robots and Systems (IROS). IEEE
- Kim G, Choi S, Kim A (2021) Scan context++: structural place recognition robust to rotation and lateral variations in urban environments. *IEEE Trans Rob* 38:1856–1874
- Kim G, Yun S, Kim J, Kim A (2022) Sc-lidar-slam: a front-end agnostic versatile lidar slam system. In: 2022 International Conference on Electronics, Information, and Communication (ICEIC). pp 1–6
- Klenk S, Chui J, Demmel N, Cremers D (2021) Tum-vie: The tum stereo visual-inertial event dataset. In: 2021 IEEE/RSJ International Conference on Intelligent Robots and Systems (IROS). pp 8601–8608
- Knapitsch A, Park J, Zhou Q-Y, Koltun V (2017) Tanks and temples: benchmarking large-scale scene reconstruction. *ACM Trans Graph (ToG)* 36:1–13
- Koval A, Karlsson S, Mansouri SS, Kanellakis C, Tevetzidis I, Haluska J, Agha-mohammadi A, Nikolakopoulos G (2022) Dataset collection from a SubT environment. *Rob Auton Syst* 155:104168. <https://doi.org/10.1016/j.robot.2022.104168>
- Kramer A, Harlow K, Williams C, Heckman C (2022) ColoRadar: the direct 3D millimeter wave radar dataset. *Int J Rob Res* 41:351–360
- Krátký V, Petrůček P, Bába T, Saska M (2021) An autonomous unmanned aerial vehicle system for fast exploration of large complex indoor environments. *J Field Robot* 38:1036–1058
- Lague D, Brodu N, Leroux J (2013) Accurate 3D comparison of complex topography with terrestrial laser scanner: application to the Rangitikei canyon (NZ). *ISPRS J Photogramm Remote Sens* 82:10–26
- Leung K, Lühr D, Houshian H, Inostroza F, Borrmann D, Adams M, Nüchter A, del Solar J (2017) Chilean underground mine dataset. *Int J Rob Res* 36:16–23
- Liu Y, Fu Y, Chen F, Goossens Bart and Tao W, Zhao H (2021) Simultaneous Localization and Mapping related datasets: a comprehensive survey. arXiv preprint [arXiv:2102.04036](https://arxiv.org/abs/2102.04036)
- Liu Y, Fu Y, Qin M, Xu Y, Xu B, Chen F, Goossens B, Yu H, Liu C, Chen L, Tao W, Zhao H (2023) BotanicGarden: A high-quality and large-scale robot navigation dataset in challenging natural environments. arXiv preprint [arXiv:2306.14137](https://arxiv.org/abs/2306.14137)
- Macario Barros A, Michel M, Moline Y, Corre G, Carrel F (2022) A comprehensive survey of visual SLAM algorithms. *Robotics*. <https://doi.org/10.3390/robotics11010024>
- Masiero A, Fissore F, Guarnieri A, Pirotti F, Visintini D, Vettore A (2018) Performance evaluation of two indoor mapping systems: low-cost UWB-aided photogrammetry and backpack laser scanning. *Appl Sci*. <https://doi.org/10.3390/app8030416>
- Menna F, Torresani A, Battisti R, Nocerino E, Remondino F (2022) A modular and low-cost portable VSLAM system for real-time 3D mapping: from indoor and outdoor spaces to underwater environments. *Int Arch Photogramm Remote Sens Spat Inf Sci* 48:153–162
- Nocerino E, Menna F, Remondino F, Toschi I, Rodr'iguez-González P (2017) Investigation of indoor and outdoor performance of two portable mobile mapping systems. In: *Videometrics, Range Imaging, and Applications XIV*. pp 125–139
- Nüchter A, Elseberg J, Janotta P (2017) Towards Mobile Mapping of Underground Mines. In: Benndorf J, Buxton M (eds) *Proceedings of Real Time Mining - International Raw Materials Extraction Innovation Conference*. TU Bergakademie Freiberg, Amsterdam, pp 27–37
- Petracek P, Kratky V, Petrlik M, Baca T, Kratochvil R, Saska M (2021) Large-scale exploration of cave environments by unmanned aerial vehicles. *IEEE Robot Autom Lett* 6:7596–7603
- Quigley M, Conley K, Gerkey B, Faust J, Foote T, Leibs J, Wheeler R, Ng AY, others (2009) ROS: an open-source Robot Operating System. In: *ICRA workshop on open source software*. pp 5–10
- Reinke A, Palieri M, Morrell B, Chang Y, Ebadi K, Carlone L, Agha-Mohammadi A-A (2022) LOCUS 2.0: robust and computationally efficient lidar odometry for real-time 3D mapping. *IEEE Robot Autom Lett* 7:9043–9050
- Ren Z, Wang L, Bi L (2019) Robust GICP-based 3D LiDAR SLAM for underground mining environment. *Sensors* 19:2915
- RIEGL Laser Measurement Systems GmbH (2019) RiSCAN PRO Operating & Processing Software
- Riegl VZ-400i Datasheet (2019) http://www.riegl.com/uploads/tx_xpriedl/downloads/RIEGL_VZ-400i_Datasheet_2022-09-27.pdf. Accessed 30 Aug 2023
- Rogers JG, Gregory JM, Fink J, Stump E (2020) Test Your SLAM! The SubT-Tunnel dataset and metric for mapping. In: 2020 IEEE International Conference on Robotics and Automation (ICRA). IEEE
- Schops T, Schonberger JL, Galliani S, Sattler T, Schindler K, Pollefeys M, Geiger A (2017) A multi-view stereo benchmark with high-resolution images and multi-camera videos. In: *Proceedings of the IEEE conference on computer vision and pattern recognition*. pp 3260–3269
- Schubert D, Goll T, Demmel N, Usenko V, Stuckler J, Cremers D (2018) The TUM VI benchmark for evaluating visual-inertial odometry. In: 2018 IEEE/RSJ International Conference on Intelligent Robots and Systems (IROS). IEEE
- Seetharaman G, Lakhota A, Blasch EP (2006) Unmanned vehicles come of age: the DARPA grand challenge. *Computer* 39:26–29
- Smith M, Baldwin I, Churchill W, Paul R, Newman P (2009) The new college vision and laser data set. *Int J Rob Res* 28:595–599
- Stach E, Pawłowska A, Matoga Ł (2014) The development of tourism at military-historical structures and sites—a case study of the building complexes of project riese in the owl mountains. *Pol J Sport Tour* 21:36–41

- Sturm J, Engelhard N, Endres F, Burgard W, Cremers D (2012) A benchmark for the evaluation of RGB-D SLAM systems. In: 2012 IEEE/RSJ International Conference on Intelligent Robots and Systems. IEEE
- Szrek J, Wodecki J, Błażej R, Zimroz R (2020) An inspection robot for belt conveyor maintenance in underground MineInfrared thermography for overheated idlers detection. *Appl Sci* 10:4984. <https://doi.org/10.3390/app10144984>
- Tak AN, Taghaddos H, Mousaei A, Bolourani A, Hermann U (2021) BIM-based 4D mobile crane simulation and onsite operation management. *Autom Constr* 128:103766. <https://doi.org/10.1016/j.autcon.2021.103766>
- Thrun S, Hahnel D, Ferguson D, Montemerlo M, Triebel R, Burgard W, Baker C, Omohundro Z, Thayer S, Whittaker W (2003) A system for volumetric robotic mapping of abandoned mines. In: 2003 IEEE International Conference on Robotics and Automation (Cat. No. 03CH37422). pp 4270–4275
- Torresani A, Menna F, Battisti R, Remondino F (2021) A V-SLAM guided and portable system for photogrammetric applications. *Remote Sens* 13: 2351 <https://doi.org/10.3390/rs13122351>
- Toschi I, Rodríguez-González P, Remondino F, Minto S, Orlandini S, Fuller A (2015) Accuracy evaluation of a mobile mapping system with advanced statistical methods. *Int Arch Photogramm Remote Sens Spatial Inform Sci*. <https://doi.org/10.5194/isprsarchives-XL-5-W4-245-2015>
- Toschi I, Ramos MM, Nocerino E, Menna F, Remondino F, Moe K, Poli D, Legat K, Fassi F et al (2017) Oblique photogrammetry supporting 3D urban reconstruction of complex scenarios. *Int Arch Photogramm Remote Sens Spatial Inform Sci* 42:519–526
- Tranzatto M, Dharmadhikari M, Bernreiter Lukas and Camurri M, Khattak S, Mascarich Frank and Pfreundschuh P, Wisth D, Zimmermann S, Kulkarni M, Reijgwart V, Casseau B, Homberger T, De Petris P, Ott Lionel and Tubby W, Waibel G, Nguyen H, Cadena C, Buchanan R, Wellhausen L, Khedekar N, Andersson O, Zhang L, Miki T, Dang T, Mattamala M, Montenegro M, Meyer K, Wu X, Briod A, Mueller M, Fallon M, Siegwart R, Hutter M, Alexis K (2022) Team CERBERUS wins the DARPA Subterranean Challenge: Technical overview and lessons learned. arXiv preprint [arXiv:220704914](https://arxiv.org/abs/220704914)
- Trybała P (2021) LiDAR-based Simultaneous Localization and Mapping in an underground mine in Złoty Stok, Poland. In: IOP Conference Series. Earth and Environmental Science
- Trybała P, Szrek J, Remondino F, Wodecki J, Zimroz R (2022) Calibration of a multi-sensor wheeled robot for the 3D mapping of underground mining tunnels. *Int Arch Photogramm Remote Sens Spatial Inform Sci*. <https://doi.org/10.5194/isprs-archives-xlvi-2-w2-2022-135-2022>
- Trybała P, Kasza D, Wajs J, Remondino F (2023) Comparison of low-cost handheld lidar-based slam systems for mapping underground tunnels. *Int Arch Photogramm Remote Sens Spat Inf Sci* 48:517–524
- Trzeciak M, Pluta K, Fathy Y, Alcalde L, Chee S, Bromley A, Brilakis I, Alliez P (2023) ConSLAM: construction data set for SLAM. *J Comput Civ Eng* 37:4023009
- Vallet B, Mallet C (2016) 2—urban scene analysis with Mobile mapping technology. In: Baghdadi N, Zribi M (eds) Land surface remote sensing in urban and coastal areas. Elsevier, pp 63–100
- Wang C, Wang W, Qiu Y, Hu Y, Scherer S (2020a) Visual memorability for robotic interestingness via unsupervised online learning. *Computer vision—ECCV 2020*. Springer International Publishing, Cham, pp 52–68
- Wang W, Zhu D, Wang X, Hu Y, Qiu Y, Wang C, Hu Y, Kapoor A, Scherer S (2020b) TartanAir: A dataset to push the limits of visual SLAM. In: 2020 IEEE/RSJ International Conference on Intelligent Robots and Systems (IROS). IEEE
- Xu W, Cai Y, He D, Lin J, Zhang F (2022) Fast-lid2: fast direct lidar-inertial odometry. *IEEE Trans Rob* 38:2053–2073
- Yang X, Lin X, Yao W, Ma H, Zheng J, Ma B (2022) A robust LiDAR SLAM method for underground coal mine robot with degenerated scene compensation. *Remote Sens* 15:186
- Zlot R, Bosse M (2013) Efficient large-scale 3D mobile mapping and surface reconstruction of an underground mine. In: Field and service robotics: Results of the 8th international conference. pp 479–493